

**Serveur Académique Lausannois SERVAL [serval.unil.ch](http://serval.unil.ch)**

## **Author Manuscript**

**Faculty of Biology and Medicine Publication**

**This paper has been peer-reviewed but does not include the final publisher proof-corrections or journal pagination.**

Published in final edited form as:

**Title:** Early processing in the human lateral occipital complex is highly responsive to illusory contours but not to salient regions.

**Authors:** Shpaner M, Murray MM, Foxe JJ

**Journal:** The European journal of neuroscience

**Year:** 2009 Nov

**Volume:** 30

**Issue:** 10

**Pages:** 2018-28

**DOI:** 10.1111/j.1460-9568.2009.06981.x

In the absence of a copyright statement, users should assume that standard copyright protection applies, unless the article contains an explicit statement to the contrary. In case of doubt, contact the journal publisher to verify the copyright status of an article.

Published in final edited form as:

*Eur J Neurosci.* 2009 November ; 30(10): 2018–2028. doi:10.1111/j.1460-9568.2009.06981.x.

## Early processing in human LOC is highly responsive to illusory contours but not to salient regions

Marina Shpaner<sup>1,2</sup>, Micah M. Murray<sup>3</sup>, and John J. Foxe<sup>1,2,#</sup>

<sup>1</sup>The Cognitive Neurophysiology Laboratory, Program in Cognitive Neuroscience, Departments of Psychology & Biology, The City College of the City University of New York, 138th Street & Convent Avenue, New York, New York 10031, USA <sup>2</sup>The Cognitive Neurophysiology Laboratory, Program in Cognitive Neuroscience & Schizophrenia, The Nathan S. Kline Institute for Psychiatric Research, 140 Old Orangeburg Road, Orangeburg, New York 10962, USA <sup>3</sup>Neuropsychology and Neurorehabilitation Service and Radiology Service, Centre Hospitalier Universitaire Vaudois and University of Lausanne, Nestlé Hospital, 5 Av. Pierre Decker, Lausanne 1011, Switzerland

### Abstract

Human electrophysiological studies support a model whereby sensitivity to so-called illusory contour stimuli is first seen within the lateral occipital complex. A challenge to this model posits that the lateral occipital complex is a general site for crude region-based segmentation, based on findings of equivalent hemodynamic activations in the lateral occipital complex to illusory contour and so-called salient region stimuli, a stimulus class that lacks the classic bounding contours of illusory contours. Using high-density electrical mapping of visual evoked potentials, we show that early lateral occipital cortex activity is substantially stronger to illusory contour than to salient region stimuli, while later lateral occipital complex activity is stronger to salient region than to illusory contour stimuli. Our results suggest that equivalent hemodynamic activity to illusory contour and salient region stimuli likely reflects temporally integrated responses, a result of the poor temporal resolution of hemodynamic imaging. The temporal precision of visual evoked potentials is critical for establishing viable models of completion processes and visual scene analysis. We propose that crude spatial segmentation analyses, which are insensitive to illusory contours, occur first within dorsal visual regions, not lateral occipital complex, and that initial illusory contour sensitivity is a function of the lateral occipital complex.

### Keywords

object recognition; event-related potentials; ERP; filling-in

### Introduction

The neural basis of visual segmentation and object surface completion has been extensively studied using illusory contour (IC) stimuli. Although earlier intracranial studies in animal models and human neuroimaging studies localized IC processing to the hierarchically lowest visual cortical regions of V1/V2 (Bakin *et al.*, 2000; Ffytche & Zeki, 1996; Larsson *et al.*, 1999; Lee & Nguyen, 2001; Peterhans & von der Heydt, 1989; Ramsden *et al.*, 2001; Seghier *et al.*, 2000; von der Heydt & Peterhans, 1989), more recent functional Magnetic Resonance

Imaging (fMRI) and magneto/electroencephalographic studies emphasize contributions from higher-order regions of the lateral occipital complex (LOC) (Foxye *et al.*, 2005; Halgren *et al.*, 2003; Kruggel *et al.*, 2001; Mendola *et al.*, 1999; Murray *et al.*, 2002; Murray *et al.*, 2004; Murray *et al.*, 2006; Ritzl *et al.*, 2003b). These latter studies support a model whereby IC sensitivity occurs first in the LOC with subsequent feedback and recurrent processes involving lower-tier areas V1 and V2.

A reasonable challenge to this body of research is that the LOC is not itself sensitive to illusory contours or completion processes, but rather is a general site for more crude region-based segmentation (Stanley & Rubin, 2003). Since LOC neurons pool information from large portions of the visual field, there is a possibility that the IC response observed within the LOC might instead represent a response to the whole figure rather than to the bounding contour *per se*. Borrowing a computationally cost-effective model for surface detection from the computer vision literature (e.g., Sharon *et al.*, 2000; Shi & Malik, 2000), Stanley and Rubin proposed that the LOC detects crude surfaces and that lower-tier cortices process bounding edges. To test this notion, they introduced modified Kanizsa-type IC stimuli, termed “salient region” (SR) stimuli, which lacked bounding illusory contours but still retained a “first impression of global surface.” Using fMRI, they revealed similar LOC activations for both standard IC stimuli and these modified SR stimuli, and on this basis they concluded that the LOC participates in the rapid detection of SR but is not involved in IC-specific processing. Rather, they proposed that IC processing takes place via feedback to lower-tier visual cortical areas (areas V1 and V2), although it should be noted that they did not explicitly assess activity in these regions for IC processing. This thesis is clearly a temporal one, positing a specific sequence of events that is simply beyond the temporal resolution of fMRI to resolve.

Over the past years, we have developed an electrophysiological metric of IC sensitivity and have shown that IC sensitivity occurs during the latency range of the N1 component of the visual evoked potential (VEP) (Foxye *et al.*, 2005; Murray *et al.*, 2002; Murray *et al.*, 2004; Murray *et al.*, 2006). This robust effect manifests as a more negative VEP deflection to stimuli when the inducers are oriented to form an IC than when no IC is induced, and is localized to bilateral LOC and posterior occipital areas. Hereafter, we will refer to this measure as the *IC-effect*, in keeping with the previous literature. We applied this metric to obtain the brain’s response to IC and SR stimuli. If Stanley and Rubin’s hypothesis regarding SR processing in LOC is correct, a clear set of predictions follows: initial activity in LOC should be identical for both conditions with a subsequent topographic or amplitude divergence (as the sharp “edges” are filled-in). If, on the other hand, LOC is in fact sensitive to ICs, initial LOC activity should be greater or even exclusive to the IC condition than to the SR condition.

## Materials and Methods

### Subjects

Thirteen (seven female) neurologically normal paid volunteers, aged 20-42 years (mean =  $28.5 \pm 7.7$  yrs.) participated. All subjects had normal or corrected-to-normal vision and were right-handed as assessed with the Edinburgh Handedness Inventory (Oldfield, 1971). Some of the participants who served had prior experience with ERP recordings while others were novice participants. None could be considered expert psychophysical observers. All subjects provided written informed consent, and the Institutional Review Board of the Nathan Kline Institute for Psychiatric Research approved all procedures. The study conforms to the principles outlined in the Declaration of Helsinki. Subjects received a modest monetary compensation (\$10 per hour) for their participation.

## Stimuli and Task

Stimuli were presented to subjects on a computer monitor located 92 cm away. Images appeared light gray on dark gray background. The “pacmen” inducers subtended  $2.8^\circ$ , along the  $45^\circ$  diagonals from the center at  $3.6^\circ$  eccentricity, producing illusory square shapes of  $7^\circ$  maximal height and width. This resulted in two types of experimental stimuli: 1) Kanizsa-type IC’s (Figure 1a&c) and 2) SR’s – modified IC stimuli where inducers’ shape and alignment were altered to eliminate bounding contours but retained a global impression of an enclosed region (as described in Stanley & Rubin, 2003). Inducers were oriented to either form or not form an illusory contour (“IC-in” and “IC-out,” respectively). Likewise, SR stimuli were oriented either facing inward or outward (“SR-in and “SR-out,” respectively), see Figure 1. The support ratio (actual physical length over the entire contour length) for stimuli facing inward was 0.40 (Ringach & Shapley, 1996; Shipley & Kellman, 1992).

Stimuli were presented for 200 ms with an inter-stimulus interval incrementally varying from 1 to 2.5 seconds (in 250 ms steps). On each trial, subjects responded with a simple button push to indicate the presence or absence of a “shape” (i.e., contour). Subjects reliably indicated the presence of shapes for the IC condition (94% accuracy), whereas only 34% of SR stimuli were perceived as containing a shape.<sup>1</sup> Given the low error rates with IC stimuli, behavioral data will not be discussed in any further detail here. Each block contained 40 stimuli with all stimulus conditions randomized and equally probable. All subjects completed at least 30 blocks of the experiment, with 4 subjects completing 35 blocks. Note that VEP analyses included all trials, irrespective of whether an illusory shape was perceived. The study by Stanley and Rubin (2003) does not provide psychophysical data concerning if or how often their participants observed illusory contours with their SR stimuli during the fMRI task. Rather, the authors included all trials in their analyses.

## Electrophysiological data acquisition

Continuous EEG was acquired through a Biosemi ActiveTwo system from 168 scalp electrodes, digitized at 512 Hz, and referenced to the CMS-DRL ground (which functions as a feedback loop driving the average potential of the subject, i.e. the Common Mode voltage, as close as possible to the AC reference voltage of the AD box, i.e. the amplifier zero). Epochs of continuous EEG (-200 ms before stimulus onset to 500 ms after stimulus onset) were separately averaged from each subject in response to each condition and stimulus type. An artifact rejection criterion of  $\pm 100 \mu\text{V}$  was used at all scalp sites to reject trials with excessive EMG, horizontal or vertical eye movements, and other noise transients. The average number of accepted sweeps per VEP was  $216 \pm 46$ . Data from artifact electrodes from each subject and VEP were interpolated (Perrin *et al.*, 1987) according to their individually digitized electrode positions (Polhemus Fastrak, 3DspaceDX software, Neuroscan, Inc.) and then affined to the average electrode locations across our group of subjects. The mean electrode positions were in turn used during the calculation of the lead field matrix for the source estimations below. Prior to group-averaging, VEP data were baseline corrected using the 100ms pre-stimulus period and also recalculated to the common average reference. Statistical and topographic mapping for all experiments in this study were performed on broadband data.

<sup>1</sup>While Stanley and Rubin (2004) did not have their participants perform a task during their fMRI recordings, a very basic task was introduced in the present study to ensure active viewing during the lengthy ERP recording. Murray *et al.*, (2002) previously showed that the *IC-effect* is elicited during passive viewing and Murray *et al.*, (2006) showed that drastically manipulating task-load did not impact the *IC-effect*. Thus, we were confident that any effects found would be independent of task parameters.

## Analysis Strategy

A first level of analysis was performed separately for each stimulus type (IC and SR), using point-wise paired *t*-tests between VEP responses from “in” and “out” configurations. Data were referenced to the fronto-polar site for this analysis simply to facilitate comparison with our prior work detailing the time course of illusory contour sensitivity (Murray *et al.*, 2002). For each electrode, the first time point where the *t*-test exceeded the 0.01  $\alpha$  criterion for at least 11 consecutive data points (21.5 ms at a 512 Hz digitization rate) was labeled as onset of the effects (see Guthrie & Buchwald, 1991). The results of this analysis are displayed as a “statistical cluster plot” (see Figure 2b). The x-, y-, and z- axes respectively represent time (post-stimulus onset), electrode location, and the p-value of the *t*-test (indicated by a color value) at each data point.

Our remaining analyses were based on the comparison of differential responses to “in” and “out” configurations between stimulus types, using a set of analyses based on local and global measures of the electric field at the scalp. These analyses and their advantages over canonical VEP waveform analyses have been discussed in detail elsewhere (e.g., Michel *et al.*, 2001; Michel *et al.*, 2004). These analyses provide a statistically-based differentiation of effects that follow from modulation in the strength of responses of statistically indistinguishable brain generators from those that are the consequence of alterations in the configuration of these generators (viz. the topography of the electric field at the scalp).

The global response strength of the electric field was analyzed using the instantaneous Global Field Power (GFP) for each subject and stimulus type. GFP is equivalent to the spatial standard deviation of the scalp electric field (Lehmann & Skrandies, 1980), and is calculated as the square root of the mean of the squared value recorded at each electrode (versus the average reference). GFP measures are used to minimize observer bias and provide a more concise view of the data. While different sources of electrical activity do not preclude identical GFP waveforms, identical topographic modulations with different GFP amplitudes can be parsimoniously interpreted as a modulation in the response strength within statistically indistinguishable configurations of underlying generators, as has been repeatedly demonstrated in prior investigations of illusory contour processes related to the difference between in and out configurations (Pegna *et al.*, 2002; Murray *et al.*, 2004 and 2006; Foxe *et al.*, 2005). Like the analysis of individual VEP waveforms represented in the statistical cluster plots, GFP waveforms were analyzed using a millisecond-by-millisecond paired *t*-test with an  $\alpha$  criterion of 0.01 and a temporal constraint of a significant difference being observed for at least 11 contiguous data points.

Differences in response topography were statistically assessed using Global Dissimilarity (Lehmann & Skrandies, 1980), which is quantified as the square root of the mean of the squared difference between the potentials measured at each electrode (vs. the average reference), each of which is first scaled to unitary strength by dividing by the instantaneous GFP. Global Dissimilarity is therefore an index of configuration differences between two electric fields, independent of their strength. It can range from 0 to 2, where 0 indicates topographic homogeneity and 2 indicates topographic inversion between responses to different stimulus types. A Monte Carlo non-parametric bootstrapping procedure (Manly, 1997), termed topography analysis of variance or TANOVA, was used to identify statistical differences between each pair of stimulus types and was furthermore conducted as a function of time (Murray *et al.*, 2008). Because electric field changes are indicative of changes in the underlying generator configuration (e.g., Fender, 1987; Lehmann, 1987); this test provides a statistical means of determining if and when the brain network activated by IC and SR stimulus types differ. As above, we applied an  $\alpha$  criterion of 0.01 and an 11-point temporal criterion.

Finally, intracranial sources of the “in” versus “out” difference were estimated for each stimulus type and subject using the local auto-regressive average (LAURA) distributed linear inverse solution (Grave de Peralta *et al.*, 2001; Grave de Peralta *et al.*, 2004), which selects the best source configuration based on the biophysical behavior of electric vector fields according to electromagnetic laws (i.e. activity at one point depends on the activity at neighboring points according to electromagnetic laws detailed in Maxwell’s equations). The version of LAURA used here employs a realistic head model with 3005 nodes arranged within the gray matter of the Montreal Neurological Institute’s average brain. This implementation of LAURA was generated with the Spherical Model with Anatomical Constraints (SMAC; Spinelli *et al.*, 2000). Time periods for source estimations were chosen based on the above topographic analyses. As will be detailed below, two time periods were identified (154-203ms and 404-469ms). Mean differences in source estimations for each of these periods were calculated and then used to identify clusters of nodes for statistical analyses. A minimal spatial extent of 5 contiguous nodes was used and each included node had a mean scalar value of at least 50% of the maximal difference. A paired t-test on the un-subtracted values was performed on the mean scalar values across nodes within identified clusters.

## Results

Previous research from our group has established an electrophysiological metric of illusory contour sensitivity the – *IC effect* – that is calculated as the VEP difference between inducer configurations that produce an illusory contour and those that do not. We applied this metric in the present study and calculated VEP differences for each stimulus class (i.e. IC and SR) by subtracting “out” (pacmen facing outward, not forming a contour) from the “in” (pacmen facing inward, forming a contour) conditions. Unsubtracted VEP waveforms from a set of exemplar posterior scalp locations situated at the maxima of the N1 topography are displayed in Figure 2a. Consistent with our prior studies, visual inspection of these group-averaged VEPs revealed a clear difference between “in” and “out” conditions that peaked during the N1 component at ~170ms post-stimulus onset. This modulation was prominent for IC, but not for SR stimuli. A first level of analysis was performed in order to facilitate comparison with our prior study that identified the spatio-temporal dynamics of Kanizsa-type illusory contour processing (Murray *et al.*, 2002). These analyses entailed a series of timepoint-by-timepoint paired t-tests between “in” and “out” conditions in response to each stimulus type (see Figure 2b and Materials and Methods for details). These statistical cluster plots indicate that IC stimuli resulted in a robust *IC effect* beginning at ~140-150ms, whereas SR stimuli did not produce the same effect. The general latency and morphology of the IC-effect is highly consistent with previous findings (e.g. Murray *et al.*, 2002, 2004, 2006; Foxe *et al.*, 2005).

To quantitatively assess commonalities and differences between stimulus types, we calculated VEP difference waveforms and conducted electrical imaging analyses on these differences. Difference waveforms at identical scalp locations to those depicted in Figure 2a are shown in Figure 3a. These locations are situated at the maxima of the “in” versus “out” difference across stimulus types, the topography of which is shown in Figure 4b. Visual inspection of these difference waveforms as well as the statistical cluster plots across the electrode montage (Figure 3b) revealed 2 general time periods of differential responses; one over the approximately 150-300ms time period and the other over the approximately 400-500ms time period. Specifically, there was a larger “in” vs. “out” differential response to IC stimuli over the earlier time period and a larger “in” vs. “out” differential response to SR stimuli over the later time period. Difference wave area measures over the 154-203 ms post-stimulus interval were submitted to a 2x2x2 repeated measures MANOVA, using stimulus type, hemiscalp, and electrode position as within subjects factors. Time periods for

these statistical tests were defined based on the topographic analyses described above. There was a significant main effect of stimulus type ( $F_{(1,11)}=13.898$ ;  $p=0.003$ ), with higher differential effect of the IC than the SR condition. No other main effect and no interaction reached the 0.05 significance criterion. Identical analyses were conducted for the later time period, 404-469ms post-stimulus. There was a significant main effect of stimulus type ( $F_{(1,11)}=28.046$ ;  $p<0.001$ ), with higher differential effect of the SR than the IC condition. The three way interaction between stimulus type, hemisphere and electrode also reached significance ( $F_{(1,11)}=6.533$ ;  $p=0.027$ ), suggestive of the different topographies for the two conditions over this time period that we detail below. No other main effect and no interaction reached the 0.05 significance criterion.

To better identify the neural generators underlying VEP differences between stimulus types, we first analyzed the Global Field Power (GFP) to assess modulations in response strength (see Figure 4a). A millisecond-by-millisecond t-test compared these waveforms, and temporally sustained differences were obtained over the 180-258ms and 275-328ms post-stimulus intervals (green trace in Figure 4a). More specifically, GFP was stronger over these intervals in response to IC than SR stimuli.

The difference topography (i.e., “in” vs. “out”) of the electric field at the scalp in response to each stimulus type was also statistically compared using non-parametric analyses of Global Dissimilarity. Temporally sustained topographic differences between IC and SR stimulus types were obtained over two intervals (blue trace in Figure 4a). The first occurred over the 154-203ms post-stimulus period, and the second over the 404-469ms post-stimulus period. These topographic effects are apparent upon inspection of sequential maps of the voltage topography at the scalp for each condition (Figure 4b). Over the earlier time period, IC stimuli exhibited a more focal and left-lateralized negative distribution over the posterior scalp. Over the later time period SR stimuli exhibited a more focal and bilateral negative distribution over the posterior scalp.

Analyses to this point indicate that IC stimuli produce different effects than do SR stimuli, with the initial “in” vs. “out” difference being considerably stronger in magnitude and different topographically. This pattern runs contrary to what would be predicted if the previously reported *IC effect* simply indexed sensitivity to salient regions of visual space. Finally, group-averaged source estimations were calculated over the 154-203ms and 404-469ms post-stimulus intervals for each stimulus type (i.e., IC and SR “in-out” difference) and are shown in Figure 5a and 5b, respectively.

Over the 154-203ms period, IC resulted in robust source estimations within the medial occipital cortex, the lateral occipital cortex, and inferior temporal cortex. By contrast, source estimations for SR stimuli were limited to the medial occipital cortex, with no evidence of strong sources within either lateral occipital or inferior temporal cortices. For both stimulus types, source estimations were stronger within the left hemisphere, consistent with the topography of the VEP (see Figure 4b). The mean difference between source estimations over the 154-203ms period is shown in the right panel of Figure 5a and illustrates that IC, but not SR stimuli, led to robust responses within the LOC (particularly within the left hemisphere; see clusters number 1 and 2). The Talairach and Tournoux (1988) coordinates of the maximal difference (SR-IC) in the left and right hemisphere were -52, -52, -8 mm and 51, -54, -3mm, respectively. These clusters extend across Brodmann’s areas (BAs) 37 and 19. Statistical analysis of the mean scalar values from nodes identified within these clusters (see Methods for details) revealed that this cortical activation was stronger in the IC conditions for the left hemisphere cluster ( $t_{(12)}=3.65$ ;  $p<0.0035$ ) and with a non-significant trend for the right hemisphere cluster ( $t_{(12)}=1.78$ ;  $p=0.10$ ), reflecting stronger contributions from sources in the LOC (Figure 5c).

Over the 404-469ms period, both IC and SR resulted in strong sources within medial occipital cortices, lateral occipital cortices, and inferior temporal cortices. Additional weaker sources were evident within the inferior parietal cortex (Figure 5b). The mean difference between source estimations over this period is shown in the right panel of Figure 5b and illustrates that IC lead to stronger sources in left LOC, whereas SR lead to stronger sources in right LOC (clusters 3 and 4, respectively). The Talairach and Tournoux (1988) coordinates of the maximal difference (SR-IC) in the left and right hemisphere were -43, -68, -3 mm and 57, -53, -3mm, respectively. These clusters extend across Brodmann's areas (BAs) 37 and 19. Statistical analysis of the mean scalar values from nodes identified within these clusters revealed no reliable difference within the left hemisphere cluster ( $t_{(12)}=1.06$ ;  $p>0.30$ ) and stronger responses in the SR condition within the right hemisphere cluster ( $t_{(12)}=2.40$ ;  $p<0.035$ ; see Figure 5c).

## Discussion

The results of this study confirm those of previous studies showing initial IC sensitivity in the human LOC during the latency range of the N1 component (e.g., Foxe *et al.*, 2005; Halgren *et al.*, 2003; Kruggel *et al.*, 2001; Murray *et al.*, 2002; Murray *et al.*, 2004; Murray *et al.*, 2006) and clearly argue against the proposition that crude region-based segmentation is the initial common stage for IC and SR processing in the LOC (Stanley & Rubin, 2003). Topographies during the N1 period were statistically different between IC and SR conditions starting around 150 ms and indicative of differences in the configuration of intracranial generators. Source estimations of the active generators during this period of visual completion were localized to higher-tier visual areas bilaterally within the ventral stream LOC, with stronger LOC sources in the IC condition (see Murray *et al.*, 2002; Sehatpour *et al.*, 2006). Over a later time period, LOC sources were stronger in the SR condition.

## Predictions of the Salient Region Hypothesis

In the present study, we assessed the extent to which there were common mechanisms for IC and SR processing. Applying the Stanley and Rubin (2003) hypothesis to the VEP methodology, the clear prediction is that initial IC and SR effects should be identical in timing, locus and mechanism (reflecting the initial common sensitivity to salient regions within the LOC). Further, their model predicts that differences between IC and SR stimulus processing will emerge later in the lower-level cortical areas (V1/V2). In contrast, if the LOC is selectively responsive to illusory contours themselves, as we have previously proposed (Foxe *et al.*, 2005; Murray *et al.*, 2006), we should observe a stronger initial response to IC stimuli within the LOC. Under such circumstances, the topography of IC and SR responses could be identical (or different). The latter prediction is precisely the pattern of responses we observed. The initial period of specific sensitivity to ICs within the LOC (as evidenced by a substantially stronger differential response between “in” and “out” conditions to ICs than to SRs) was also marked by a significant topographic difference between IC and SR responses, with the IC response relying more heavily on ventral stream sources than the SR response. We also conducted analyses of a later time period between 400 and 480 ms to provide an alternative explanation for the fMRI results observed by Stanley and Rubin (2003). Responses were of greater amplitude over occipital electrodes to SR stimuli during this later processing stage, possibly accounting for the equivalent fMRI activations between the conditions. That is, because the BOLD response measured using fMRI pools activity within a region over time, effects over the early and late timeframes are summed to produce equal IC and SR responses.

When VEP waveforms are considered in isolation, one could argue that the results of the present study indicate a quantitative rather than a qualitative difference between the two



conditions. However, topographical analyses and source estimations clearly show that areas of the brain, specifically the LOC, are engaged differentially for the IC and the SR stimuli in the timeframe of N1.

Additional evidence against the salient region hypothesis can be gleaned from an earlier fMRI investigation that included stimulus conditions wherein illusory contours were induced by displaced line gratings, which unlike Kanizsa-type stimuli lack salient regions (c.f. Figure 1 of Mendola *et al.*, 1999). In this study, Mendola and colleagues observed the strongest differential responses to displaced versus control stimuli within the LOC. These results suggest that the illusory contour perception modulates LOC activity rather than information conveyed by line ends or salient regions. The present results provide further support for the LOC model of illusory contour processing and argue against the LOC model of rapid detection of salient regions.

### Implications for the “identity hypothesis”

The results of the present study are also germane to a recent and often heated debate in the literature over the mechanisms of so-called modal and amodal<sup>2</sup> contour completion (see e.g. Anderson, 2007; Kellman *et al.*, 2007). Kellman and colleagues (2005) have argued that the two classes of stimuli share a common initial mechanism for generating contour connections across space - the so-called “identity hypothesis.” In response, Anderson (2007) has argued on the basis of single-cell recording studies (e.g., Bakin *et al.*, 2000; Lee & Nguyen, 2001) that modal and amodal stimuli do not share common mechanisms, in that these studies show differential responses in hierarchically early cortical regions. However, our series of studies has demonstrated that these differences in early cortical regions (i.e. V1 and V2) likely stem from feedback from higher order visual areas (Murray *et al.*, 2002, 2004, 2006; Foxe *et al.*, 2005), thus reflecting a later perceptual mechanism (see also Lamme and Spekreijse, 2000). Further, Murray and colleagues (2004) demonstrated identical initial electrophysiological responses to modal and amodal stimuli in human observers. That is, we found identical *IC-effects* for both stimulus classes, and that these effects originated in the LOC bilaterally. Anderson dismissed these findings, stating that it was “*highly unlikely that the identical responses observed by Murray et al. (2004) have anything to do with contour interpolation processes*”, basing this assertion on the findings of Stanley and Rubin (2003). That is, he asserted that the LOC could not be involved in contour interpolation given the equivalent fMRI activations in LOC for IC and SR stimuli. Clearly, this latter argument is not supported by the results of the current study.

### Previous Event-related Potential Results

A previous study by Yoshino and colleagues (2006) compared VEP’s to IC and SR stimuli in much the same fashion as was done here; but in complete opposition to the present findings, they concluded that LOC was responsible for crude region-based segmentation with subsequent IC boundary completion. In light of the present findings, a re-consideration of their data is warranted and we contend that their conclusions are thoroughly inconsistent with their reported pattern of results. First, Yoshino and colleagues report an interaction between inducer type, inducer orientation and electrode-site during the N1 latency; a result that they interpret as showing that the N1 potential was larger for IC than the other three conditions at certain electrode sites. But this is not the correct interpretation. Rather, this interaction points to the fact that certain electrode sites had a larger difference between IC-in vs. IC-out conditions than between SR-in vs. SR-out conditions, i.e. the N1 was more sensitive to IC processing. In fact, Yoshino and colleagues rightfully conclude that IC

<sup>2</sup>Illusory contour stimuli used in the present study are modal contours (see Figure 1). Amodal contours are contours occluded by a foreground object (see Murray *et al.*, 2004 for examples).

modulation can be “extracted from [the] N1 component”. Looking at their figures 2 and 3, it is clear that the effect for ICs during N1 is substantially larger than for SRs, much like is seen here (note that the four electrodes illustrated in the present paper roughly correspond to the PO3 and PO4 electrodes analyzed by Yoshino and colleagues (2006), the electrodes which showed differential effects between IC and SR conditions).

Second, the progression of events observed by Yoshino and colleagues is very similar to the time-course of activations observed in our study. The “*IC effect*” (“in” vs. “out”) is reported to start at 70 ms post stimulus onset. The authors further report bilateral LOC sources of activation over 110-180 ms time range. The earliest topographic difference between ICs and SRs begins at 170 ms in their dataset. It follows that the earliest activity in LOC (110-170 ms) was an amplitude modulation (see interaction described above), most sensitive to IC stimuli, and stemming from identical intracranial generators. Consequently, the study of Yoshino and colleagues is fully consistent with the results of our study. As we have discussed previously, the salient-region hypothesis has to /be rejected when initial LOC activation is more sensitive to IC stimuli with or without a concurrent topographic difference between IC and SR. The former is the result observed by Yoshino and colleagues; the latter is the result observed in this study.

### Stipulating the contour detection mechanism

The results of this study are consistent with a model of IC processing in humans whereby initial IC sensitivity takes place in the lateral occipital cortex (LOC), a complex of higher order visual areas (Foxe *et al.*, 2005; Halgren *et al.*, 2003; Kruggel *et al.*, 2001; Murray *et al.*, 2002; Murray *et al.*, 2004; Murray *et al.*, 2006; Ritzl *et al.*, 2003a). This initial activity in the LOC is followed by feedback to V1/V2 and likely thereafter involves recurrent rounds of feedback and feedforward information flow between higher-tier regions with their large receptive fields and lower-tier small receptive field regions. A similar sequence of events has been very convincingly demonstrated by Lamme and colleagues using intracranial recordings in non-human primates for a related class of stimuli, so called figure-ground textures (Lamme & Spekreijse, 2000). Interestingly, an fMRI study of IC processing reported higher V1 activity and a simultaneous decrease in LOC activity as a result of perceptual learning (Maertens & Pollmann, 2005). The authors proposed that initially IC processing relied heavily on LOC, whereas, with learning, local connections in V1 were strengthened. The later sweep of activity in the LOC (here around 400-500ms) represents more effortful perceptual closure mechanisms, previously implicated in object-recognition for difficult-to-recognize fragmented objects and also in illusory contour studies (Doniger *et al.*, 2000; Doniger *et al.*, 2002; Murray *et al.*, 2002; Sehatpour *et al.*, 2006; Sehatpour *et al.*, 2008).

While we agree with Stanley and Rubin (2003) that contour integration processes must be preceded by a more general spatial segmentation process, we show that this general segmentation process does not rely on the LOC. Rather, our results are more consistent with the “frame-and-fill” theory of visual processing (Chen *et al.*, 2006). This theory maintains that an initial “framing” of the scene is processed by structures of the dorsal visual stream, which in turn feeds into ventral stream structures, where the slower parvocellular system “fills in” the details (Bar, 2003; for similar models see Vidyasagar, 1999). Crude region-based segmentation can be viewed as a form of spatial processing, more consistent with the functions of the dorsal stream (e.g., Mishkin *et al.*, 1982). Due to the rapid nature of the magnocellular dorsal pathways, crude region-based segmentation is expected to happen relatively early after stimulus onset and earlier than the N1 timeframe (e.g., Chen *et al.*, 2006), likely during the earlier P1 latency (65-100ms). Dorsal stream generators have been shown to contribute substantially to the P1 component (Di Russo *et al.*, 2002; Foxe *et al.*, 2001; Foxe *et al.*, 2005), and the P1 is well-known to be responsive to spatial attentional

manipulations (e.g., Hillyard & Mangun, 1987; Martinez *et al.*, 1999). Consistent with this notion, Murray *et al.* (2002) described P1 sensitivity to the spatial distribution of their IC inducers (the pacmen). P1 amplitude systematically increased as the eccentricity of the inducers increased. Importantly, this effect was independent of the presence vs. absence of illusory contours; identical effects were obtained for outwardly and inwardly turned inducers. In the present study, no differences in brain activation were observed prior to the N1 timeframe, as all stimulus types (both inward and outward facing pacmen) could be considered as equally effective in delineating the spatial extent of the scene. VEP studies directly manipulating spatial aspects of the scene will clearly be necessary to further test this interpretation.

In conclusion, our data show that LOC is considerably more sensitive to illusory contour stimuli than salient region stimuli during early sensory-perceptual processing as measured with temporally precise electrophysiological methods in humans. These results suggest that prior fMRI evidence of equivalent IC and SR responses within the LOC likely reflects temporally-integrated responses. We reject the hypothesis that the common process of spatial segmentation takes place in LOC and, instead, propose that it is more likely to happen in the dorsal stream prior to the earliest processing in LOC.

## Acknowledgments

This work was supported by a grant from the US National Institute of Mental Health (MH65350 to JJJ). We thank Drs. Damian Stanley and Nava Rubin for kindly providing their original stimuli for this study. MS received support from a City University of New York (CUNY) Science Fellowship. MMM received support from the Swiss National Science Foundation and the Leenaards Foundation. Beth Higgins, Jeannette Mahoney and Manuel Gomez-Ramirez provided technical assistance. Cartool software (<http://brainmapping.unige.ch/Cartool.htm>) has been programmed by Denis Brunet from the Functional Brain Mapping Laboratory, Geneva, Switzerland, and is supported by the EEG Brain Mapping Core of the Center for Biomedical Imaging (CIBM) of Geneva and Lausanne.

## Reference List

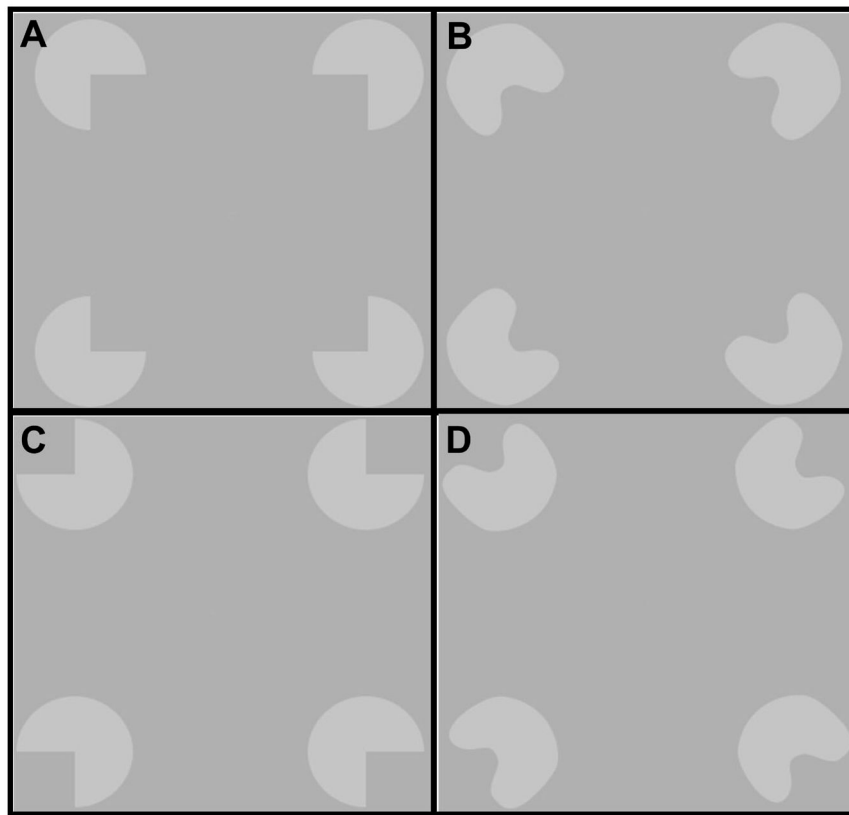
- Anderson BL. Filling-in models of completion: rejoinder to Kellman, Garrigan, Shipley, and Keane (2007) and Albert (2007). *Psychol Rev.* 2007; 114(2):509–27. [PubMed: 17500640]
- Bakin JS, Nakayama K, Gilbert CD. Visual responses in monkey areas V1 and V2 to three-dimensional surface configurations. *J Neurosci.* 2000; 20:8188–8198. [PubMed: 11050142]
- Bar M. A cortical mechanism for triggering top-down facilitation in visual object recognition. *J Cogn Neurosci.* 2003; 15:600–609. [PubMed: 12803970]
- Chen CM, Lakatos P, Shah AS, Mehta AD, Givre SJ, Javitt DC, Schroeder CE. Functional Anatomy and Interaction of Fast and Slow Visual Pathways in Macaque Monkeys. *Cereb Cortex.* 2006
- Di Russo F, Martinez A, Sereno MI, Pitzalis S, Hillyard SA. Cortical sources of the early components of the visual evoked potential. *Hum Brain Mapp.* 2002; 15:95–111. [PubMed: 11835601]
- Doniger GM, Foxe JJ, Murray MM, Higgins BA, Javitt DC. Impaired visual object recognition and dorsal/ventral stream interaction in schizophrenia. *Arch Gen Psychiatry.* 2002; 59:1011–1020. [PubMed: 12418934]
- Doniger GM, Foxe JJ, Murray MM, Higgins BA, Snodgrass JG, Schroeder CE, Javitt DC. Activation timecourse of ventral visual stream object-recognition areas: high density electrical mapping of perceptual closure processes. *J Cogn Neurosci.* 2000; 12:615–621. [PubMed: 10936914]
- Fender, DH. Methods of analysis of brain electrical and magnetic signals. In: Gevins, AS.; Remond, A., editors. *Handbook of electroencephalography and clinical neurophysiology.* Elsevier; Amsterdam: 1987. p. 355-399.
- Ffytche DH, Zeki S. Brain activity related to the perception of illusory contours. *Neuroimage.* 1996; 3:104–108. [PubMed: 9345481]
- Foxe JJ, Doniger GM, Javitt DC. Early visual processing deficits in schizophrenia: impaired P1 generation revealed by high-density electrical mapping. *Neuroreport.* 2001; 12:3815–3820. [PubMed: 11726801]

- Foxe JJ, Murray MM, Javitt DC. Filling-in in Schizophrenia: a High-density Electrical Mapping and Source-analysis Investigation of Illusory Contour Processing. *Cereb Cortex*. 2005
- Grave de Peralta MR, Gonzalez AS, Lantz G, Michel CM, Landis T. Noninvasive localization of electromagnetic epileptic activity. I. Method descriptions and simulations. *Brain Topogr*. 2001; 14:131–137. [PubMed: 11797811]
- Grave de Peralta MR, Murray MM, Michel CM, Martuzzi R, Gonzalez Andino SL. Electrical neuroimaging based on biophysical constraints. *Neuroimage*. 2004; 21:527–539. [PubMed: 14980555]
- Guthrie D, Buchwald JS. Significance testing of difference potentials. *Psychophysiology*. 1991; 28:240–244. [PubMed: 1946890]
- Halgren E, Mendola J, Chong CD, Dale AM. Cortical activation to illusory shapes as measured with magnetoencephalography. *Neuroimage*. 2003; 18:1001–1009. [PubMed: 12725774]
- Hillyard SA, Mangun GR. Sensory gating as a physiological mechanism for visual selective attention. *Electroencephalogr Clin Neurophysiol Suppl*. 1987; 40:61–67. [PubMed: 3480183]
- Kellman PJ, Garrigan P, Shipley TF. Object interpolation in three dimensions. *Psychol Rev*. 2005; 112(3):586–609. [PubMed: 16060752]
- Kellman PJ, Garrigan P, Shipley TF, Keane BP. Interpolation processes in object perception: reply to Anderson (2007). *Psychol Rev*. 2007; 114(2):488–508. [PubMed: 17500638]
- Kruggel F, Herrmann CS, Wiggins CJ, von Cramon DY. Hemodynamic and electroencephalographic responses to illusory figures: recording of the evoked potentials during functional MRI. *Neuroimage*. 2001; 14:1327–1336. [PubMed: 11707088]
- Lamme VA, Spekreijse H. Modulations of primary visual cortex activity representing attentive and conscious scene perception. *Front Biosci*. 2000; 5:D232–D243. [PubMed: 10704153]
- Larsson J, Amunts K, Gulyas B, Malikovic A, Zilles K, Roland PE. Neuronal correlates of real and illusory contour perception: functional anatomy with PET. *Eur J Neurosci*. 1999; 11:4024–4036. [PubMed: 10583491]
- Lee TS, Nguyen M. Dynamics of subjective contour formation in the early visual cortex. *Proc Natl Acad Sci U S A*. 2001; 98:1907–1911. [PubMed: 11172049]
- Lehmann, D. Principles of spatial analysis. In: Gevins, AS.; Remond, A., editors. *Methods of Analysis of Brain Electrical and Magnetic Signals Handbook of Electro-Encephalography and Clinical Neurophysiology*. Elsevier; Amsterdam: 1987. p. 309-354.
- Lehmann D, Skrandies W. Reference-free identification of components of checkerboard-evoked multichannel potential fields. *Electroencephalogr Clin Neurophysiol*. 1980; 48:609–621. [PubMed: 6155251]
- Maertens M, Pollmann S. fMRI reveals a common neural substrate of illusory and real contours in V1 after perceptual learning. *J Cogn Neurosci*. 2005; 17:1553–1564. [PubMed: 16269096]
- Manly, B.F.J. *Randomization, Bootstrap and Monte Carlo Methods in Biology*. Chpman and Hall; London: 1997.
- Martinez A, Anllo-Vento L, Sereno MI, Frank LR, Buxton RB, Dubowitz DJ, Wong EC, Hinrichs H, Heinze HJ, Hillyard SA. Involvement of striate and extrastriate visual cortical areas in spatial attention. *Nat Neurosci*. 1999; 2:364–369. [PubMed: 10204544]
- Mendola JD, Dale AM, Fischl B, Liu AK, Tootell RB. The representation of illusory and real contours in human cortical visual areas revealed by functional magnetic resonance imaging. *J Neurosci*. 1999; 19:8560–8572. [PubMed: 10493756]
- Michel CM, Murray MM, Lantz G, Gonzalez S, Spinelli L, Grave de PR. EEG source imaging. *Clin Neurophysiol*. 2004; 115:2195–2222. [PubMed: 15351361]
- Michel CM, Thut G, Morand S, Khateb A, Pegna AJ, Grave de PR, Gonzalez S, Seeck M, Landis T. Electric source imaging of human brain functions. *Brain Res Brain Res Rev*. 2001; 36:108–118. [PubMed: 11690607]
- Mishkin M, Lewis ME, Ungerleider LG. Equivalence of parieto-preoccipital subareas for visuospatial ability in monkeys. *Behav Brain Res*. 1982; 6:41–55. [PubMed: 7126324]
- Murray MM, Foxe DM, Javitt DC, Foxe JJ. Setting boundaries: brain dynamics of modal and amodal illusory shape completion in humans. *J Neurosci*. 2004; 24:6898–6903. [PubMed: 15295024]

- Murray MM, Imber ML, Javitt DC, Foxe JJ. Boundary completion is automatic and dissociable from shape discrimination. *J Neurosci*. 2006; 26:12043–12054. [PubMed: 17108178]
- Murray MM, Wylie GR, Higgins BA, Javitt DC, Schroeder CE, Foxe JJ. The spatiotemporal dynamics of illusory contour processing: combined high-density electrical mapping, source analysis, and functional magnetic resonance imaging. *J Neurosci*. 2002; 22:5055–5073. [PubMed: 12077201]
- Oldfield RC. The assessment and analysis of handedness: the Edinburgh inventory. *Neuropsychologia*. 1971; 9:97–113. [PubMed: 5146491]
- Palmer EM, Kellman PJ, Shipley TF. A theory of dynamic occluded and illusory object perception. *J Exp Psychol Gen*. 2006; 135:513–541. [PubMed: 17087570]
- Perrin F, Pernier J, Bertrand O, Giard MH, Echallier JF. Mapping of scalp potentials by surface spline interpolation. *Electroencephalogr Clin Neurophysiol*. 1987; 66:75–81. [PubMed: 2431869]
- Peterhans E, von der Heydt R. Mechanisms of contour perception in monkey visual cortex. II. Contours bridging gaps. *J Neurosci*. 1989; 9:1749–1763. [PubMed: 2723748]
- Ramsden BM, Hung CP, Roe AW. Real and illusory contour processing in area V1 of the primate: a cortical balancing act. *Cereb Cortex*. 2001; 11:648–665. [PubMed: 11415967]
- Ringach DL, Shapley R. Spatial and temporal properties of illusory contours and amodal boundary completion. *Vision Res*. 1996; 36:3037–3050. [PubMed: 8917767]
- Ritzl A, Marshall JC, Weiss PH, Zafiris O, Shah NJ, Zilles K, Fink GR. Functional anatomy and differential time courses of neural processing for explicit, inferred, and illusory contours. An event-related fMRI study. *Neuroimage*. 2003b; 19:1567–1577. [PubMed: 12948712]
- Ritzl A, Marshall JC, Weiss PH, Zafiris O, Shah NJ, Zilles K, Fink GR. Functional anatomy and differential time courses of neural processing for explicit, inferred, and illusory contours. An event-related fMRI study. *Neuroimage*. 2003a; 19:1567–1577. [PubMed: 12948712]
- Seghier M, Dojat M, on-Martin C, Rubin C, Warnking J, Segebarth C, Bullier J. Moving illusory contours activate primary visual cortex: an fMRI study. *Cereb Cortex*. 2000; 10:663–670. [PubMed: 10906313]
- Sehatpour P, Molholm S, Javitt DC, Foxe JJ. Spatiotemporal dynamics of human object recognition processing: an integrated high-density electrical mapping and functional imaging study of “closure” processes. *Neuroimage*. 2006; 29:605–618. [PubMed: 16168676]
- Sehatpour P, Molholm S, Schwartz TH, Mahoney JR, Mehta AD, Javitt DC, Stanton PK, Foxe JJ. A human intracranial study of long-range oscillatory coherence across a frontal-occipital-hippocampal brain network during visual object processing. *Proc Natl Acad Sci U S A*. 2008; 105:4399–4404. [PubMed: 18334648]
- Sharon E, Brandt A, Basri R. Fast Multiscale Image Segmentation. *Proc IEEE Conf on Computer Vision and Pattern Recognition (South Carolina)*. 2000:70–77.
- Shi J, Malik J. Normalized Cuts and Image Segmentation. *IEEE Trans Patt Anal Mach Intel*. 2000; 22:888–905.
- Shipley TF, Kellman PJ. The role of discontinuities in the perception of subjective figures. *Percept Psychophys*. 1990; 48:259–270. [PubMed: 2216653]
- Shipley TF, Kellman PJ. Strength of visual interpolation depends on the ratio of physically specified to total edge length. *Percept Psychophys*. 1992; 52(1):97–106. [PubMed: 1635860]
- Stanley DA, Rubin N. fMRI activation in response to illusory contours and salient regions in the human lateral occipital complex. *Neuron*. 2003; 37:323–331. [PubMed: 12546826]
- Talairach, J.; Tournoux, P. *Co-Planar Stereotaxic Atlas of the Human Brain*. Thieme; New York: 1988.
- Vidyasagar TR. A neuronal model of attentional spotlight: parietal guiding the temporal. *Brain Res Brain Res Rev*. 1999; 30:66–76. [PubMed: 10407126]
- von der Heydt R, Peterhans E. Mechanisms of contour perception in monkey visual cortex. I. Lines of pattern discontinuity. *J Neurosci*. 1989; 9:1731–1748. [PubMed: 2723747]
- Yoshino A, Kawamoto M, Yoshida T, Kobayashi N, Shigemura J, Takahashi Y, Nomura S. Activation time course of responses to illusory contours and salient region: a high-density electrical mapping comparison. *Brain Res*. 2006; 1071:137–144. [PubMed: 16413507]

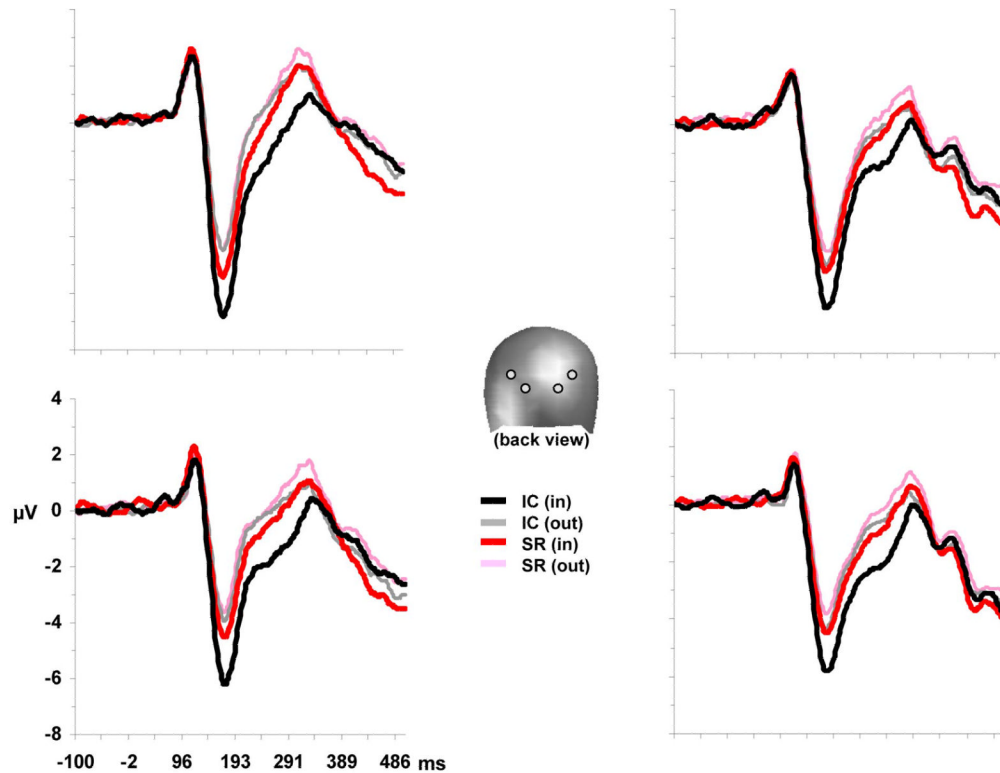
## Abbreviations

<b>fMRI</b>	functional Magnetic Resonance Imaging
<b>GFP</b>	Global Field Power
<b>IC</b>	Illusory Contours
<b>LAURA</b>	local auto-regressive average
<b>LOC</b>	Lateral Occipital Complex
<b>SR</b>	Salient Regions
<b>VEP</b>	Visual Evoked Potentials

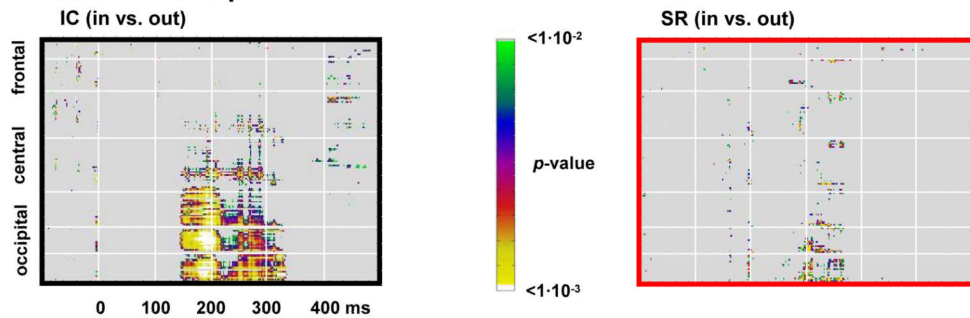


**Figure 1.** Illustration of the stimuli. (a) IC-forming stimulus; to be viewed at 30 cm distance to simulate experimental conditions (i.e., 7° illusory contour), IN configuration. (b) SR-forming stimulus; to be viewed at 30 cm distance, IN configuration. (c) Control stimulus for the IC condition, OUT configuration. (d) Control stimulus for the SR condition, OUT configuration.

## a. Exemplar VEP waveforms



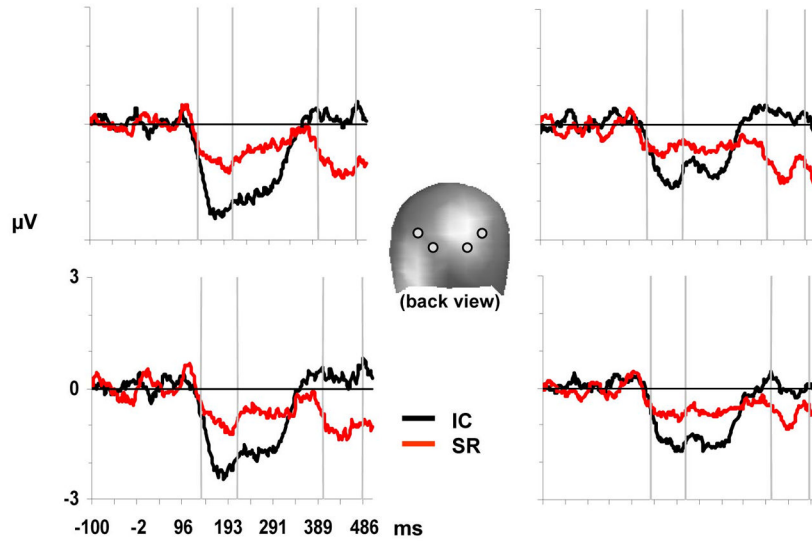
## b. Statistical cluster plots

**Figure 2.**

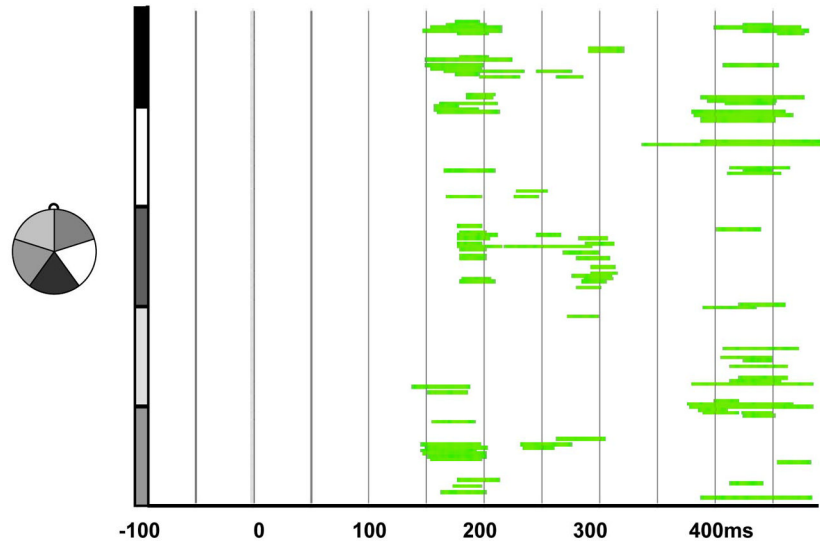
Electrophysiological response to IC and SR stimuli over the entire epoch (-100 to 500ms). (a) Group-averaged VEPs for each stimulus type over four posterior scalp sites (see inset for locations and color scheme). (b) Point-wise paired *t*-tests (“statistical cluster plots”) comparing IN (pacmen facing in) vs. OUT (pacmen facing out) configurations of the three inducer types ( $p=0.01$  threshold, over -100 to 500 ms time period). Color represents the result of the *t*-test. Electrodes are arranged left to right for seven scalp regions, demarcated by solid white lines: occipital, parieto-occipital, parietal, central, fronto-central, frontal, and fronto-polar.



### a. VEP difference waveforms

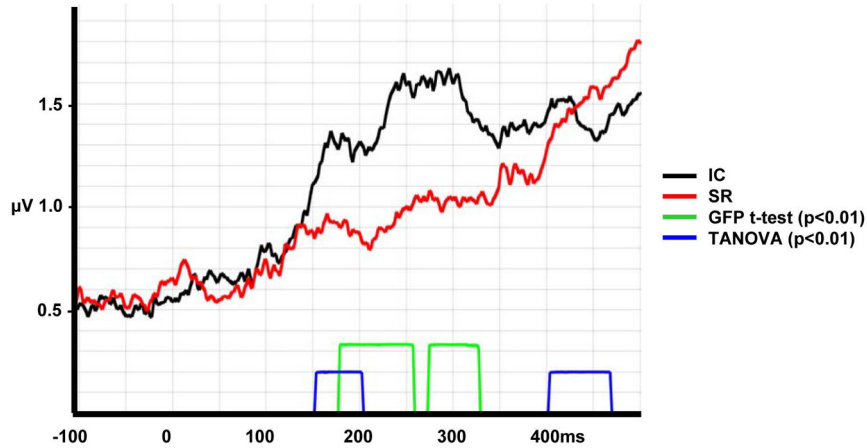


### b. Statistical cluster plot (IC vs. SR difference waveforms)

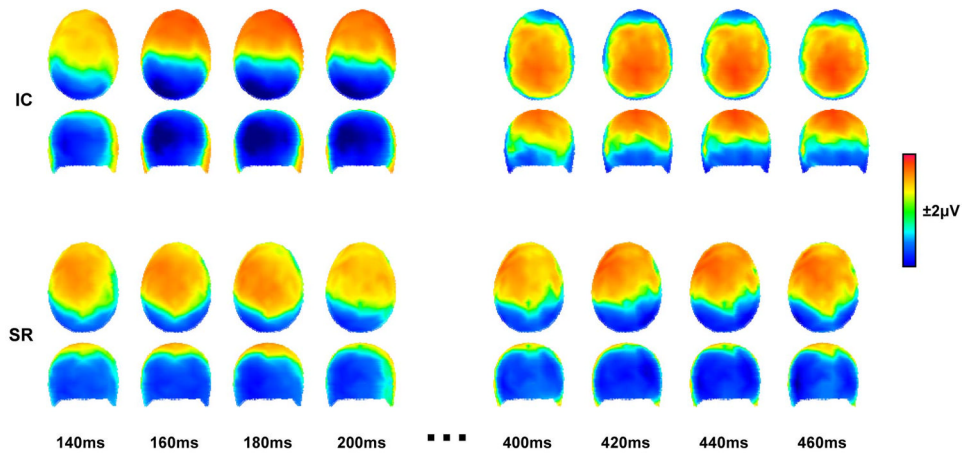


**Figure 3.** VEP difference waveforms (IN-OUT) to IC and SR stimuli over the entire epoch (-100 to 500ms). (a) Group-averaged VEP difference waveforms over four posterior electrodes (see inset for locations and color scheme). Vertical lines indicate time periods of interest (154-203ms and 404-469ms). (b) Point-wise paired *t*-tests (“statistical cluster plots”) comparing IC difference vs. SR difference responses ( $p=0.01$  threshold, over -100 to 500 ms time period). Electrodes are arranged into five scalp regions along the vertical axis; regions are displayed to the left of the plot.

## a. GFP difference waveforms, analysis &amp; TANOVA results

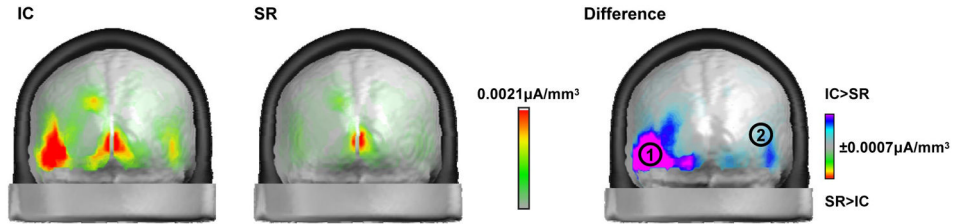


## b. VEP difference topographies

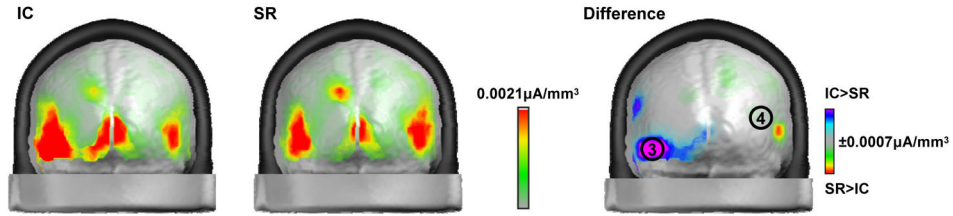
**Figure 4.**

Electrical imaging results. (a) Group-average global field power (GFP) waveforms (see inset for the color scheme). Time-periods of significant GFP *t*-test and TANOVA analyses are demarcated on the x-axis. The TANOVA analysis compared response topography between difference waveforms (IN-OUT) for the two stimulus types as a function of time. Time intervals of significant ( $p < 0.01$ ) topographic difference using a non-parametric Monte Carlo bootstrapping procedure are displayed. (b) VEP difference waveform topographies for the two conditions.

a. Group-averaged source estimations (154-203ms)



b. Group-averaged source estimations (404-469ms)



c. Mean scalar values within clusters

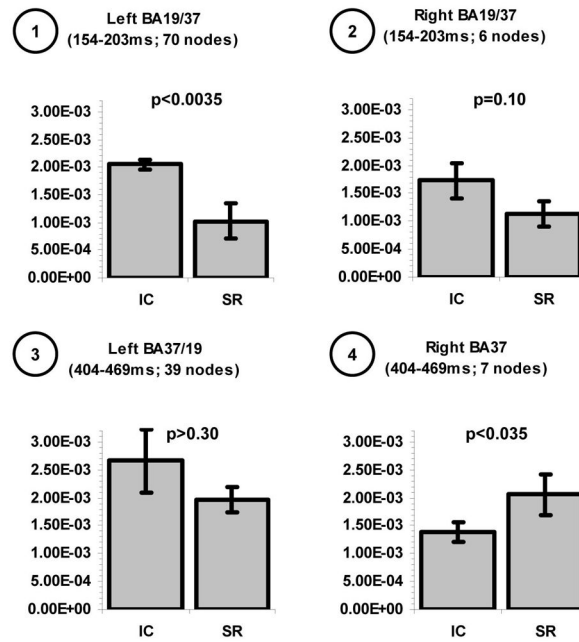


**Figure 5.**

Source estimations. Group-averaged LAURA distributed linear source estimations were calculated for the VEP difference waveforms over the 154-203ms time period (panel a) and the 404-469ms time period (panel b). The mean differences between these source estimations are shown in the right column. Significantly stronger contributions from LOC sources were found in the early time period for the IC condition (left Brodmann's area 19/37, cluster 1) and in the later time period for the SR condition (right Brodmann's area 37, cluster 4). (c) Mean scalar values of activations within clusters and *t*-test results between conditions.